https://doi.org/10.5194/gmd-2020-348
Preprint. Discussion started: 5 November 2020

Geoscientific Model Development Discussions

Effects of black carbon morphology on the brown carbon absorption estimation: from numerical aspects

Jie Luo, Yongming Zhang, and Qixing Zhang

State Key Laboratory of Fire Science, University of Science and Technology of China, Hefei, Anhui 230026, China

Correspondence: Qixing Zhang (qixing@ustc.edu.cn)

Abstract. In this work, we developed a numerical method to investigate the effects of black carbon morphology on the estimation of brown carbon (BrC) absorption using the Absorption Ångström exponent (AAE) method. Pseudo measurements of the total absorption were generated based on several morphologically mixed black carbon (BC) models, then the BrC absorption was inferred based on different AAE methods. By comparing the estimated BrC absorption with "True" BrC absorption, we found that both AAE=1 and Mie AAE methods do not provide accurate estimation for the BrC absorption, and the estimated BrC absorption can deviate several times from "True" BrC absorption. The newly proposed Wavelength Dependent AAE (WDA) method does not necessarily improve the estimations, sometimes it may even provide worse estimations than the AAE=1 and Mie AAE methods. Fixing the fractal dimension to be 1.8, the deviation between the estimated BrC mass absorption cross-section (MAC) and "True" BrC MAC can reach approximately 9 m^2/g, which is far more than brown carbon MAC itself. Therefore, the estimation of BrC absorption based on the AAE method should carefully consider the morphological effects of BC. Our findings highlight the BC morphological effects on the BrC absorption estimation.

1 Introduction

Carbonaceous aerosols, a main source of the light-absorbing aerosols, contribute great effects on the climate. Carbonaceous aerosols mainly include black carbon (BC) and organic carbon (OC). BC was considered as the dominant absorbing aerosol in the atmosphere, which greatly absorbs light from ultraviolet (UV) wavelengths to near-infrared wavelengths, and it contributes to large warming effects on the climate (Stocker et al., 2013). OC was often regarded as a scattering aerosol, while many studies have shown that parts of OC can also strongly absorb light in UV wavelengths (Kirchstetter et al., 2004; Chakrabarty et al., 2010; Chen and Bond, 2010), and the absorbing OC is called brown carbon (BrC). To figure out the climate effects of BrC, many modeling studies have been studied. BrC was estimated to contribute to approximately 20-40% of the total aerosol absorption, and its direct radiative effect has been estimated to be comparable to that of BC (Feng et al., 2013; Saleh et al., 2015). However, substantial uncertainties exist in the climate modeling of BrC (Wang et al., 2016). The accurate estimation of BrC demands the constraints from the observation.

Laboratory measurements based on the extraction of filter samples were widely used to measure BrC absorption, while it is difficult to provide global, continuous measurements. Thus, increasing studies used measurements based on remote sensing and in-situ techniques. However, the observed absorptions are commonly from the mixing of different aerosols. To divide the

https://doi.org/10.5194/gmd-2020-348
Preprint. Discussion started: 5 November 2020

Geoscientific Model Development Discussions

contributions of different aerosols, some attempts were made to derive the BrC contribution from the total absorption (Wang et al., 2016, 2018; Russell et al., 2010; Massabò et al., 2015; Bahadur et al., 2012; Chung et al., 2012). Dust, BC, and BrC are widely accepted to be the main absorbing aerosols in the atmosphere. Dust is recognized to be in the coarse mode, while BrC and BC are commonly in fine size mode. Therefore, based on the size information inferred from remote sensing using different techniques (eg. The extinction Ångström exponent (EAE)), the dust and other absorbing aerosols can be divided. However, it is difficult to divide BC and BrC based on the size information. To quantify the absorption contribution of BrC in the fine mode, a typical method was commonly used based on the strong spectral-dependence of BrC from UV to near-infrared wavelengths. BrC is commonly seen to be non-absorbing in the near-infrared wavelengths, so the fine aerosol total absorption in near-infrared wavelengths is completely from BC absorption (exclude the dust). In UV wavelengths, the total absorption should be the sum of BrC and BC absorption. Therefore, BrC absorption is the difference between the total absorption and BC absorption. Therefore, the derivation of the BrC absorption suffers large uncertainties from BC properties. The most widely used method is based on the absorption Ångström exponent (AAE), which represents the spectral dependence of the absorption. Given two wavelengths (λ_1 and λ_2), the AAE at the corresponding wavelength pair can be calculated using:

$$AAE = -\frac{ln(\frac{abs(\lambda_1)}{abs(\lambda_2)})}{ln(\frac{\lambda_1}{\lambda_2})} \quad (1)$$

where $abs(\lambda_1)$ and $abs(\lambda_2)$ represent the absorptions at λ_1 and λ_2, respectively. Given the AAE value of BC, the BC absorption in UV wavelengths can be obtained based on the absorption in near-infrared wavelengths. However, there are large uncertainties in the estimation of BC AAE. AAE=1 is widely assumed, while the particle size, morphology, and mixing states have significant impacts on BC AAE values (Kirchstetter et al., 2004; Schnaiter et al., 2003; Li et al., 2016; Liu et al., 2018; Zhang et al., 2020; Liu and Mishchenko, 2018). For example, for bare BC, Schnaiter et al. (2003) reported an average AAE value of approximately 1.1 for diesel BC aerosols; Kirchstetter et al. (2004) have shown BC AAE was approximately 0.6-1.3 for BC near the roadway or in the tunnel. Recent studies have realized that BC morphology, particle size, and mixing states can lead to sizable uncertainties in BC AAE (Li et al., 2016; Lack and Cappa, 2010; Liu et al., 2018; Luo et al., 2020). A recent study conducted by Wang et al. (2016) used the Mie calculation to constrain the effects of particle size on the AAE, while a spherical BC morphology was assumed. In their study, a pre-calculated wavelength-dependence of AAE (WDA) based on Mie calculation was used, while the effects of BC morphology was not considered. In the atmosphere, BC presents rather complex morphologies based on the observation of electron microscopy (EM) images (China et al., 2013; Wang et al., 2017). To estimate BrC absorption based on measurements from satellite or ground-based measurements, previous studies have developed some techniques to constrain the aerosol refractive index and aerosol type (Tesche et al., 2011; Arola et al., 2011). However, most studies have neglected the effects of BC morphologies. Even though recent studies have also shown BC morphologies can affect BC AAE, few studies have provided direct evidence on how large uncertainties BC morphologies can cause for the estimation of BrC absorption. Therefore, we need to answer a question: Can BC morphologies be ignored in the estimation of BrC absorption?

As measurements in the atmosphere are caused by many factors including particle size, refractive index, mixing states, morphologies, etc., it is difficult to figure out how BC morphologies affect BrC absorption derivation. In addition, it is hard to

https://doi.org/10.5194/gmd-2020-348
Preprint. Discussion started: 5 November 2020


Geoscientific Model Development Discussions

quantify the uncertainties due to the effects of aerosol composition and size distributions (Li, Z. and Zhao, X. and Kahn, R. and Mishchenko, M. and Remer, L. and Lee, K.-H. and Wang, M. and Laszlo, I. and Nakajima, T. and Maring, H., 2009). To answer the question proposed above, we need a well-constrained measurement. Numerical tools have an edge on revealing the complex factors that affect the measurements and can be the supplements for the measurements. In this work, we replace the complex measurements in the atmosphere with the well-constrained pseudo absorption "measurements" computed using morphologically realistic mixed models, and the inferred BrC absorptions based on the AAE=1, Mie AAE, and Mie wavelength-dependent AAE methods were compared with the "True" BrC absorption. Also, the causes of the uncertainties were analyzed, and the method used in this work is shown in Figure 1. Our results can provide suggestions for the estimation of BrC absorption based on multiple wavelengths.

2 Pseudo measurements

2.1 Morphologies

Non-spherical aerosol models show more excellent performance on reproducing the measurements even though Mie theory was commonly used in remote sensing and climate modeling (Bi et al., 2018; He et al., 2016, 2015; Chakrabarty et al., 2007; Luo et al., 2019). In the atmosphere, BC can be mixed with BrC, and the mixing states are commonly divided into externally mixed and internally mixed. For the externally mixed particles, each chemical component is separated, and the BrC and BC absorption can be treated individually. However, BC and BrC are well mixed for internally mixed particles. As BC is internally mixed with BrC, the total absorption can be enhanced by the "lensing effect "(Bond and Bergstrom, 2006; Lack et al., 2009) or weakened by the "sunglass effect" (Luo et al., 2018b).

The pseudo measured absorptions were calculated based on the morphologically realistic BC models. For the externally mixed particles, a fractal morphology was assumed for BC, and the structures satisfy the fractal law (Mishchenko et al., 2002):

$$N_s = k_0(\frac{R_g}{R})^{D_f} \tag{2}$$

where N_s and R represent the monomer number and mean monomer radius, respectively; D_f denote the fractal dimension, and larger D_f generally represents more compact aggregates. k_0 represents the fractal frefator, and it mainly affects the shape anisotropy. R_g represents the gyration radius. To generate BC aggregates, a tunable algorithm was applied (Woźniak, 2012).

Similar to Luo et al. (2018b), a constant monomer radius of 20 nm was assumed. As both fluffy and compact BC exist in the atmosphere, we use $D_f = 1.8$ and $D_f = 2.6$ to represent the fluffy and compact BC, respectively. As k_0 has fewer effects on the BC radiative properties (Liu and Mishchenko, 2005), we fixed k_0 to be 1.2. According to Zhang et al. (2008), we used mobility diameters of 155 nm and 320 nm to represent small and large BC, respectively. As BC shape is irregular, we substitute volume-mean BC diameter ($D_V = 2a(N_s)^{1/3}$) for the mobility diameter. The corresponding N_s are 58 and 512, respectively. The morphology of BrC was assumed to be spherical, as externally mixed BrC commonly exists as the spherical tarballs

https://doi.org/10.5194/gmd-2020-348
Preprint. Discussion started: 5 November 2020


Geoscientific Model Development Discussions

(Chakrabarty et al., 2010). We assume BC refractive index to be 1.85+0.71i (Bond and Bergstrom, 2006), and the real part of the BrC refractive index was assumed to be 1.55 (Chakrabarty et al., 2010).

For the internally mixing particles, the BC-containing morphologies were generated based on the models proposed by Luo et al. (2019). Two coating methods were assumed. The first coating method is controlled by a parameter k. In this study, $k = 8$ was assumed, and the generated BC model was referred to as Model A. The second coating method is dominated by a defined parameter (R_c). $R_c = 50R_g$ and $R_c = R_g$ were assumed to represent the film and spherical coatings, and are named Model B and Model C, respectively. In our previous study (Luo et al., 2019), we have demonstrated that our proposed models can greatly simulate the internally mixed BC morphologies and reproduce the measured absorption as well. For more details about the algorithm to generate the coated BC, please refer to Luo et al. (2019), and the typically generated morphologies are shown in Figure 2 and the Figures S1-S2 of Luo et al. (2019).

2.2 Generation of pseudo measurements

For the externally mixed particles, the absorption efficiencies (Q_{abs}) of BC and BrC were calculated using the multiple-sphere T-matrix (MSTM) method (Mackowski and Mishchenko, 2011, 1996), while the discrete dipole approximation (DDA) method was used to produce the absorption efficiencies of internally mixed particles. In this work, we used DDSCAT version 7.3 (Draine and Flatau, 2008, 1994), and we assumed the particles are randomly orientated (Mishchenko and Yurkin, 2017). After the absorption efficiencies were calculated, the absorption cross-section can be obtained using:

$$C_{abs} = \frac{1}{4} Q_{abs} \pi D_V^2 \tag{3}$$

In real circumstances, the total absorptions can be inferred from the observations or measurements. Thus, the total absorption cross-section was used to provide pseudo measurements. For the internally mixed particles, the total absorption cross-section can be directly obtained from the calculations based on the morphologically realistic models. For the externally mixed particles, the total absorption cross-section is the sum of the absorption cross-section of BC and BrC.

3 Inferring the BrC absorption

3.1 "True" BrC absorption

In the study of Luo et al. (2018b), by separating the absorption of BC and BrC, they found the total absorption of the internally mixed particles can be less than the sum of BrC and BC absorption calculated individually. So, there must be a negative effect to weaken the total absorption. From physical points, they found the BrC absorption can block the solar radiation deeply into BC, so weaken the total absorption. In addition, the "lensing effect" was redefined as the absorption enhancements of BC by the addition of non-absorbing coating materials. Therefore, the total absorptions of mixed particles consist of BC absorption, BrC absorption, the "lensing effect, and the "sunglass effect". However, both the sunglass effect and BrC shell absorption are caused by absorbing BrC. For convenient application, the "True" BrC absorption was assumed as the difference between the absorption of BC mixed with BrC and BC mixed with non-absorbing materials. Here we must clarify that the "True" BrC

https://doi.org/10.5194/gmd-2020-348
Preprint. Discussion started: 5 November 2020


Geoscientific Model Development Discussions

absorption in this work is the co-effect of the absorption BrC shell and the sunglass effect for internally mixed particles. To eliminate the effect of BrC mass, the BrC mass absorption cross-section (MAC_{BrC}) was used, and it can be calculated using:

$$C_{abs\_BrC} = C_{abs\_BC\ and\ BrC} - C_{abs\_BC\ and\ non-absorbing} \tag{4}$$

$$MAC_{BrC} = C_{abs\_BrC}/M_{BrC} \tag{5}$$

here $C_{abs\_BC\ and\ BrC}$ and $C_{abs\_BC\ and\ non-absorbing}$ represent the absorption cross-sections of BC mixed with BrC and non-absorbing materials, respectively. The morphologies of BC mixed with non-absorbing materials is the same as those mixed with BrC ; M_{BrC} represents the mass of BrC, which was calculated using:

$$M_{BrC} = V_{BrC} \cdot \rho_{BrC} \tag{6}$$

$$V_{BrC} = V_{BC} . (1 - f_{BC})/f_{BC} \tag{7}$$

$$V_{BC} = Ns . (4/3\pi R^3) \tag{8}$$

where V_{BrC} and V_{BC} represent the volume of BrC and BC, respectively; f_{BC} represents the volume fraction of BC; ρ_{BrC} represents the mass density of BrC, and it was assumed to be 1.2 g/cm^3 as Luo et al. (2018b).

As the BrC absorption estimation is significantly affected by the BC physical properties, we have also calculated the difference between "True" and the estimated BC absorption by assuming BC is mixed with non-absorbing materials. However, as the difference between "True" and the estimated BC absorption mainly affect the estimation of BrC absorption, the absorption difference was normalized by BrC mass but not BC mass. Here we used a parameter δ_{MAC} to represent the difference of "True" and the estimated BrC absorption:

$$\delta_{C_{abs}} = C_{abs\_BC\_Ture} - C_{abs\_BC\_inferred} \tag{9}$$

$$\delta_{MAC} = \delta_{C_{abs}}/M_{BrC} \tag{10}$$

where $C_{abs\_BC\_Ture}$ and $C_{abs\_BC\_inferred}$ ρ_{BC} represent the "True" and inferred absorption cross-sections of BC mixed with non-absorbing materials. As the BrC MAC deviation between "Ture" and inferred BrC absorption is mainly caused by the inaccurate estimation of BC absorption, δ_{MAC} can represent the deviation between the "True" and inferred BrC MAC.

https://doi.org/10.5194/gmd-2020-348
Preprint. Discussion started: 5 November 2020


Geoscientific Model Development Discussions

3.2 Inferring BrC absorption

The calculation of inferred BrC absorption is similar to the true case, while the difference is the $C_{abs\_BC\ and\ non-absorbing}$ is inferred from an assumed AAE:

$$C_{abs\_BC\_non-absorbing2} = C_{abs\_BC\_non-absorbing1} \cdot (\frac{\lambda_2}{\lambda_1})^{-AAE} \tag{11}$$

here $C_{abs\_BC\_non-absorbing1}$ and $C_{abs\_BC\_non-absorbing2}$ are the corresponding absorption cross-section of BC with non-absorbing materials at λ_1 and λ_2, respectively.

The total absorptions observation at 440, 675, 870 nm can be commonly obtained in AERONET and other ground measurements. Based on the strong spectral-dependence of BrC, BrC absorption at 675 and 870 nm wavelengths are commonly neglected, and the absorption at 675 and 870 nm are fully from the BC absorption. As BC absorption at 440 nm wavelength can be obtained based on the BC AAE, we can estimate the BrC absorption at 440 nm based on Equation 1. In this work, we inferred the mass absorption cross-section (MAC) of BrC at 440 nm wavelength based on the pseudo measurements at 675 and 870 nm wavelength using AAE=1 and AAE of Mie calculations.

In addition, Wang et al. (2016) proposed a method to derive BrC absorption based on AAE spectral-dependence (WDA) using Mie calculations. The WDA was calculated using:

$$WDA = AAE_{\lambda1\_\lambda2} - AAE_{\lambda2\_\lambda3} \tag{12}$$

where $AAE_{\lambda1\_\lambda2}$ and $AAE_{\lambda2\_\lambda3}$ are AAE calculated using different wavelength pairs. Based on the different size and refractive index, the WDA was pre-calculated by performing Mie calculations, and then the AAE at a wavelength pair is inferred from AAE observation at another wavelength pair and precalculated WDA. As for the spherical BC, the optical properties are also calculated using MSTM but not Mie method to eliminate the errors caused by different numerical methods. However, the deviation between MSTM and Mie method for spherical BC should not be large. In this work, the WDA is calculated using MSTM by assuming a spherical morphology, and then the AAE between UV and near-infrared wavelengths are inferred from WDA and AAE in near-infrared wavelengths. Take the wavelengths of 440 nm,675 nm and 870 nm for example, AAE between 440 nm and 675 nm can be calculated using:

$$WDA = AAE_{440nm\_870nm\_Mie} - AAE_{675nm\_870nm\_Mie} \tag{13}$$

$$AAE_{440nm\_870nm\_inferred} = AAE_{675nm\_870nm\_True} + WDA \tag{14}$$

In this work, for the inverse of BrC absorption, all the WDA is calculated based on the Mie theory, and we call it the WDA method. We have also demonstrated the effects of morphologies on the applicability of the WDA method.

https://doi.org/10.5194/gmd-2020-348
Preprint. Discussion started: 5 November 2020

Geoscientific Model Development Discussions

4 Results

4.1 Externally mixed particles

The BrC mass absorption cross-section is significantly depending on the imaginary part of the BrC refractive index. The measured imaginary parts of BrC refractive indices were varied largely in different pieces of literature. For example, Nakayama et al. (2013) showed that the secondary OC generated from the photooxidation of toluene has an imaginary part of refractive index from 0 to 0.0082 and from 0-0.0017 at 405 nm and 532 nm respectively; Saleh et al. (2013) showed that the imaginary part of primary OC refractive indices was in the range of 0.0055-0.06, while the imaginary parts of secondary OC refractive indices varied in the range of 0.01-0.05. Even though the imaginary part of BrC refractive indices suffer large uncertainties in chemical compositions, aging status, and generating process, the reported value commonly within the range between the values reported by Kirchstetter et al. (2004) and those reported by Chen and Bond (2010). In general, the measured imaginary part of the BrC refractive index commonly within the range of approximately 0-0.16.

The measured BrC mass absorption cross-section was also varied in different studies. The range of from 1.26 to 1.79 m^2/g at 365 nm wavelength was reported by previous studies (Cheng et al., 2011; Du et al., 2014; Srinivas et al., 2016). Cho et al. (2019) reported a mean BrC mass absorption cross-section of approximately 0.7 m^2/g at 565 nm. BrC absorption properties based on laboratory measurements in urban and biomass smoke samples at Lawrence Berkeley National Laboratory showed BrC mass absorption cross-section of 2.75, 0.95, 0.42, 0.32, and 0.21 at λ= 400, 500, 600, 700, and 900 nm, respectively. In this work, the "True" BrC mass absorption cross-sections are generally within the range of approximately 0-4m^2/g when varying the imaginary part of the BrC refractive index. Our calculated BrC mass absorption cross-section range is a little wider than the measurements as the wide imaginary part range of BrC refractive index was assumed.

The comparisons of the "True" and inferred BrC absorption for externally mixed particles are shown in Figure 3. In general, the inferred mass BrC absorption agrees relatively well with the "True" BrC absorption when BC fraction is small. This is easy to be understood. The total effects caused by the BC morphology are alleviated by the large BrC fraction, so the effects of BC morphology on the inferred mass BrC absorption is small. However, as the ratio of BC volume to BrC volume reaches 1:1, the inferred mass BrC absorption based on the AAE method may be significantly affected by the BC morphology. For the large particle, the Mie AAE method may provide inaccurate estimations for both fluffy and compact particles, and the Mie AAE method can overestimate the BrC mass absorption by approximately 4.8 m^2/g, which is approximately several times of the observed BrC absorption. For small particles, the effects of BC morphologies on the Mie AAE method is relatively small. However, this is also non-negligible, as the Mie AAE method may underestimate the BrC absorption for about 0.5-1 m^2/g when f_{BC}=50%, which is comparable to the observed BrC absorption. As the morphological effects on the BrC absorption derivation are significantly dependent on the particle size, we have also investigated δ_{MAC} at different particle sizes. As shown in Figure 4, the accuracy of the Mie AAE method is significantly dependent on the particle size. Fixing D_f to be 1.8, δ_{MAC} can increase with D_V, and δ_{MAC} can reach approximately 4.8 m^2/g when the particle size is large. The different accuracy of the Mie AAE method for small and large particles is due to the different dependency of BC AAE on the particle size for spherical and fractal BC. As shown in Figure 5, spherical BC AAE is significantly dependent on the particle size, and the AAE

https://doi.org/10.5194/gmd-2020-348
Preprint. Discussion started: 5 November 2020


Geoscientific Model Development Discussions

can reach a negative value for large BC. However, for fractal BC aggregates, the AAE is still about 1 for large BC, so the Mie AAE method provides rather inaccurate estimations for large particles.

The applicability of the AAE=1 method should be also carefully considered. By assuming the AAE to be 1, the BrC mass absorption cross-section can be underestimated. Even though BrC MAC is relative accurately estimated for small particles, when the particle is large, fixing f_{BC}=50%, most BrC mass absorption cross-section inferred by assuming AAE=1 is below 0. Even though the AAE=1 method can provide reasonable estimations for fluffy aggregates (also see Figure 4), as BC becomes compact, the underestimation of BrC MAC can reach approximately 2.3 m^2/g. The reason is that bare BC AAE is still approximately 1 for fluffy aggregates (see Figure 5), while the AAE of large compact BC can be approximately 0.7 (Liu et al., 2018). Therefore, the use of the AAE=1 method should carefully consider both the particle size and BC morphologies.

To dispose of the effects of particle size on the AAE method, Wang et al. (2016) proposed a method based on the WDA method to derive BrC absorption. However, the WDA method does not necessarily provide a better estimation than using the AAE=1, as the BC morphology in the atmosphere is rather complex. As shown in Figure 3, assuming that the BC morphology present fractal characteristics, the WDA method may provide worse estimations than using the AAE=1 for small particles. As shown in Figure 4, the accuracy of the WDA method is significantly dependent on the particle size. As D_V is approximately 100 nm, BrC MAC can be underestimated by approximately 9 m^2/g using the WDA method. This may be due to that the Mie WDA method overestimates the effects of particle size. To compare the WDA of spherical BC and fractal BC, we have calculated the WDA of fractal aggregates with D_V varying from 40 to 400 nm based on the calculated database from our previous work (Luo et al., 2018a), where the BC refractive index was assumed to be $m = 1.95 + 0.79i$. As shown in Figure 5, WDA of spherical BC is largely dependent on the particle size, while the WDA of fractal aggregates does not deviate largely with zero. Therefore, the effects of BC morphologies on the applicability of the WDA method should be carefully considered. In addition, we also notice that even though the "True" BrC absorption is larger than 0, the inferred BrC absorption can be below 0 as the BC contents become large. Therefore, we should carefully consider the BC contents when using the AAE method to estimate the BrC absorption.

4.2 Internally mixed particles

As BC and BrC are internally mixed, the morphologies become more complex. Not only the fractal parameters (such as D_f) may change, but also the coating configuration may affect the morphologies. To demonstrate the effect of morphologies, we use three BC models based on different coating configurations to calculate the absorption of the internally mixed particles, as referred above. As shown in Figure 6, different BrC coating shapes may lead to sizable uncertainties in the "True" BrC absorption. Fixing BrC refractive index to be 1.55+0.08i, the uncertainties in the BrC mass absorption cross-section caused by different BrC coating shapes can vary from 0 to approximately 0.25 m^2/g. In addition, the particle size and compactness of mixed particles can also have significant effects on BrC absorption. Therefore, the determination of BrC absorption based on the modeling method should consider the variation of BrC coating shapes for internally mixed BrC even though most externally mixed BrC presents a near-spherical shape.

https://doi.org/10.5194/gmd-2020-348
Preprint. Discussion started: 5 November 2020


Geoscientific Model Development Discussions

For internally mixed particles, the comparisons of "True" BrC MAC and the inferred BrC MAC are shown in Figure 7. The "True" BrC MAC derived from internally mixed assumption is a little smaller than that of externally mixed particles due to the blocking effects of absorbing coating materials. The inferred BrC MAC also deviates largely from the "True" BrC MAC for internally mixed particles. The inferred BrC MAC based on the Mie AAE method may deviate more largely from "True" BrC MAC compared to the externally mixed particles. Fixing N_s to be 512, and D_f to be 1.8, the inferred BrC MAC using the Mie AAE at 440 and 870 nm wavelength pair can overestimate the "True" BrC MAC by approximately 5.8 m^2/g. As also shown in Figure 8, fixing D_f to be 1.8, δ_{MAC} based on the Mie AAE method is not very large when the particle is small, while it increases to approximately 5.8 m^2/g when the D_V of the mixed particles increases to approximately 400 nm. Furthermore, even for heavily coated BC (f_{BC}=10%), the Mie AAE method can overestimate the BrC MAC by approximately 1.0 m^2/g (see both Figure 7 and Figure 8), which is comparable to the BrC MAC. Therefore, the applicability of the Mie AAE method is significantly limited by BC morphologies when the particle is large.

The WDA method may even provide worse estimations than the AAE=1 method for small particles. Fixing N_s to be 58 and f_{BC} to be 50%, the WDA method can overestimate BrC MAC by approximately 2 m^2/g, which is comparable to "True" BrC MAC. As shown in Figure 8, fixing D_f to be 1.8, as the particle size of the mixed particles increases, δ_{MAC} based on the WDA method increases firstly and then decreases. The WDA method can overestimate the BrC MAC by approximately 2.5 m^2/g when D_V of the mixed particles is approximately 200 nm. The reason may be that the WDA calculated using the Mie method overestimates the effect of the BC size. As shown in Figure 9, even though the WDA of Model A does not deviate largely with 0, the WDA of the core-shell sphere model depends largely on the particle size. So the Mie WDA can overestimate the effects of the particle size, and the WDA method is extremely limited by the BC morphologies.

The performance of the AAE=1 method is also significantly constrained by the BC morphology. For the fluffy internally thinly coated BC, BC AAE is still around 1 (see Figure 9), so the estimation of BrC MAC using the AAE=1 method is reasonable. However, for large BC, as BC becomes compact, the AAE method can underestimate the BrC MAC by 2-3 m^2/g. The possible reason may be that AAE of more compact BC deviate larger with 1 when BC size is large, as demonstrated in the study of Liu et al. (2018). The inferred BrC absorption based on the Mie AAE provides rather inaccurate estimations, and the deviation with the pseudo measurements can reach approximately 1.2 m^2/g even for f_{BC}=10%. The reason is that the Mie AAE method can provide inaccurate estimations for "True" AAE. Figure 9 shows that the AAE of the core-shell sphere model can deviate more largely with 1 compared to Model A. Especially for large particles, Mie AAE can significantly underestimate the "True" AAE, so significantly overestimate BrC MAC. Therefore, the BrC absorption derivation should carefully consider the effects of BC morphologies.

To constrain the uncertainties caused by the BC morphologies, BC morphological information obtained from electron microscopy sampling in different conditions can be used. For example, by exploring the three-dimensional (3D) electron tomography method, Adachi et al. (2007) have analyzed the morphological characteristics of BC. Based on the two-dimensional (2D) electron tomography image and fractal theory, China et al. (2013) have characterized the BC structures emitted from the wildfire. BC structures in the freeway were also analyzed by China et al. (2014). Besides, Yuan et al. (2019) have investigated

https://doi.org/10.5194/gmd-2020-348
Preprint. Discussion started: 5 November 2020


Geoscientific Model Development Discussions
Open Access
EGU

the externally mixed and internally mixed BC at a remote site in the Southeastern Tibetan Plateau. These measurements can provide morphological information for constraining the uncertainties in the estimation of the BrC absorption.

5 Conclusions

In this work, the effects of BC morphologies on the derivation of BrC absorption based on the AAE method were numerically investigated. To focus on the effects of BC morphologies, pseudo measurements were generated based on some morphological mixed BC models, then the BrC absorption was inferred based on the AAE method. By comparing the inferred BrC absorption with "True" BrC absorption, we found the applicability of the AAE method is severely affected by the BC morphologies. Even though the "True" BrC absorption is within the measured range, the inferred BrC absorption can be even less than 0 as the BC volume fraction increases. The Mie AAE method does not provide an accurate estimation for most particles due to the overestimation of the size effects on AAE. For both externally and internally mixed particles, the AAE=1 method is severely limited by the BC morphology, and the deviation with the "True" BrC absorption can vary from near 0 to several times more than the "True" BrC absorption. The WDA method does not necessarily improve the estimations. In many cases, the WDA method even provides worse estimation than the AAE=1 method, and the deviation of BrC MAC can reach approximately 9 m^2/g for externally mixed particles. Therefore, the estimation of BrC absorption based on the AAE method should carefully consider the effects of BC morphologies. This work highlights the BC morphological effects on the BrC absorption estimation, and it can provide suggestions for the estimation of BrC absorption.

Data availability. The data used in this work can be found at https://figshare.com/articles/dataset/Deriving_BrC_Revised_zip/12839570 (Luo, 2020).

Author contributions. JL and QZ conceived the research idea. JL performed the computations, and wrote the paper. YZ verified the simulation methods and results. QZ reviewed the paper and supervised the findings of this work. All authors discussed the results and contributed to the final paper.

Competing interests. The authors declare that no competing interests.

Acknowledgements. We thank the fund support of the National Natural Science Foundation of China (Grant No. 41675024 and U1733126); Fundamental Research Funds for the Central Universities (Grant No. WK2320000040). We particularly thank Dr. D. W. Mackowski and Dr. M. I. Mishchenko for the MSTM code, and thank Bruce Draine and Pjotr Flatau for the DDSCAT software. We also acknowledge the support of super computing center of University of Scenice and Technology of China.

https://doi.org/10.5194/gmd-2020-348
Preprint. Discussion started: 5 November 2020

Geoscientific Model Development Discussions

References

Adachi, K., Chung, S. H., Friedrich, H., and Buseck, P. R.: Fractal parameters of individual soot particles determined using electron tomography: Implications for optical properties, Journal of Geophysical Research: Atmospheres, 112, 2007.

Arola, A., Schuster, G., Myhre, G., Kazadzis, S., Dey, S., and Tripathi, S. N.: Inferring absorbing organic carbon content from AERONET data, Atmospheric Chemistry and Physics, 11, 215–225, https://doi.org/10.5194/acp-11-215-2011, https://www.atmos-chem-phys.net/11/215/2011/, 2011.

Bahadur, R., Praveen, P. S., Xu, Y., and Ramanathan, V.: Solar absorption by elemental and brown carbon determined from spectral observations, Proceedings of the National Academy of Sciences, 109, 17 366–17 371, 2012.

Bi, L., Lin, W., Wang, Z., Tang, X., Zhang, X., and Yi, B.: Optical Modeling of Sea Salt Aerosols: The Effects of Nonsphericity and Inhomogeneity, Journal of Geophysical Research: Atmospheres, 123, 543–558, https://doi.org/10.1002/2017JD027869, https://agupubs.onlinelibrary.wiley.com/doi/abs/10.1002/2017JD027869, 2018.

Bond, T. C. and Bergstrom, R. W.: Light absorption by carbonaceous particles: An investigative review, Aerosol Science and Technology, 40, 27–67, https://doi.org/10.1080/02786820500421521, <GotoISI>://WOS:000233906000001, 2006.

Chakrabarty, R., Moosmüller, H., Chen, L.-W., Lewis, K., Arnott, W., Mazzoleni, C., Dubey, M., Wold, C., Hao, W., and Kreidenweis, S.: Brown carbon in tar balls from smoldering biomass combustion, Atmospheric Chemistry and Physics, 10, 6363–6370, 2010.

Chakrabarty, R. K., Moosmüller, H., Arnott, W. P., Garro, M. A., Slowik, J. G., Cross, E. S., Han, J.-H., Davidovits, P., Onasch, T. B., and Worsnop, D. R.: Light scattering and absorption by fractal-like carbonaceous chain aggregates: comparison of theories and experiment, Applied Optics, 46, 6990–7006, https://doi.org/10.1364/AO.46.006990, http://ao.osa.org/abstract.cfm?URI=ao-46-28-6990, 2007.

Chen, Y. and Bond, T.: Light absorption by organic carbon from wood combustion, Atmospheric Chemistry and Physics, 10, 1773–1787, 2010.

Cheng, Y., He, K.-B., Zheng, M., Duan, F.-K., Du, Z.-Y., Ma, Y.-L., Tan, J.-H., Yang, F.-M., Liu, J.-M., Zhang, X.-L., et al.: Mass absorption efficiency of elemental carbon and water-soluble organic carbon in Beijing, China, Atmospheric Chemistry and Physics, 11, 11 497–11 510, 2011.

China, S., Mazzoleni, C., Gorkowski, K., Aiken, A. C., and Dubey, M. K.: Morphology and mixing state of individual freshly emitted wildfire carbonaceous particles, Nature Communications, 4, <GotoISI>://WOS:000323715900002, 2013.

China, S., Salvadori, N., and Mazzoleni, C.: Effect of Traffic and Driving Characteristics on Morphology of Atmospheric Soot Particles at Freeway On-Ramps, Environmental Science and Technology, 48, 3128–3135, <GotoISI>://WOS:000333776000007, 2014.

Cho, C., Kim, S.-W., Lee, M., Lim, S., Fang, W., Örjan Gustafsson, Andersson, A., Park, R. J., and Sheridan, P. J.: "Observation-based estimates of the mass absorption cross-section of black and Brown carbon and their contribution to aerosol light absorption in East Asia", Atmospheric Environment, https://doi.org/https://doi.org/10.1016/j.atmosenv.2019.05.024, http://www.sciencedirect.com/science/article/pii/S135223101930319X, 2019.

Chung, C. E., Ramanathan, V., and Decremer, D.: Observationally constrained estimates of carbonaceous aerosol radiative forcing, Proceedings of the National Academy of Sciences, 109, 11 624–11 629, 2012.

Draine, B. T. and Flatau, P. J.: Discrete-Dipole Approximation for Scattering Calculations, Journal of the Optical Society of America a-Optics Image Science and Vision, 11, 1491–1499, <GotoISI>://WOS:A1994NE24300032, 1994.

Draine, B. T. and Flatau, P. J.: Discrete-dipole approximation for periodic targets: theory and tests, Journal of the Optical Society of America a-Optics Image Science and Vision, 25, 2693–2703, <GotoISI>://WOS:000261520700009, 2008.

https://doi.org/10.5194/gmd-2020-348
Preprint. Discussion started: 5 November 2020

Geoscientific Model Development Discussions

Du, Z., He, K., Cheng, Y., Duan, F., Ma, Y., Liu, J., Zhang, X., Zheng, M., and Weber, R.: "A yearlong study of water-soluble organic carbon in Beijing II: Light absorption properties", Atmospheric Environment, 89, 235 – 241, https://doi.org/https://doi.org/10.1016/j.atmosenv.2014.02.022, http://www.sciencedirect.com/science/article/pii/S1352231014001186, 2014.

Feng, Y., Ramanathan, V., and Kotamarthi, V.: Brown carbon: a significant atmospheric absorber of solar radiation?, Atmospheric Chemistry and Physics, 13, 8607–8621, 2013.

He, C., Liou, K.-N., Takano, Y., Zhang, R., Levy Zamora, M., Yang, P., Li, Q., and Leung, L. R.: Variation of the radiative properties during black carbon aging: theoretical and experimental intercomparison, Atmospheric Chemistry and Physics, 15, 11 967–11 980, https://doi.org/10.5194/acp-15-11967-2015, https://www.atmos-chem-phys.net/15/11967/2015/, 2015.

He, C., Takano, Y., Liou, K.-N., Yang, P., Li, Q., and Mackowski, D. W.: "Intercomparison of the GOS approach, superposition T-matrix method, and laboratory measurements for black carbon optical properties during aging", Journal of Quantitative Spectroscopy and Radiative Transfer, 184, 287 – 296, https://doi.org/https://doi.org/10.1016/j.jqsrt.2016.08.004, http://www.sciencedirect.com/science/article/pii/S0022407316303879, 2016.

Kirchstetter, T. W., Novakov, T., and Hobbs, P. V.: Evidence that the spectral dependence of light absorption by aerosols is affected by organic carbon, Journal of Geophysical Research-Atmospheres, 109, <GotoISI>://WOS:000225190500010, 2004.

Lack, D. A. and Cappa, C. D.: Impact of brown and clear carbon on light absorption enhancement, single scatter albedo and absorption wavelength dependence of black carbon, Atmospheric Chemistry and Physics, 10, 4207–4220, https://doi.org/10.5194/acp-10-4207-2010, https://www.atmos-chem-phys.net/10/4207/2010/, 2010.

Lack, D. A., Cappa, C. D., Cross, E. S., Massoli, P., Ahern, A. T., Davidovits, P., and Onasch, T. B.: Absorption Enhancement of Coated Absorbing Aerosols: Validation of the Photo-Acoustic Technique for Measuring the Enhancement, Aerosol Science and Technology, 43, 1006–1012, <GotoISI>://WOS:000269731800002, 2009.

Li, J., Liu, C., Yin, Y., and Kumar, K. R.: Numerical investigation on the Ångström Exponent of black carbon aerosol, Journal of Geophysical Research-Atmospheres, 121, 3506–3518, <GotoISI>://WOS:000375120200027, 2016.

Li, Z. and Zhao, X. and Kahn, R. and Mishchenko, M. and Remer, L. and Lee, K.-H. and Wang, M. and Laszlo, I. and Nakajima, T. and Maring, H.: Uncertainties in satellite remote sensing of aerosols and impact on monitoring its long-term trend: a review and perspective, Annales Geophysicae, 27, 2755–2770, https://doi.org/10.5194/angeo-27-2755-2009, https://angeo.copernicus.org/articles/27/2755/2009/, 2009.

Liu, C., Chung, C. E., Yin, Y., and Schnaiter, M.: The absorption Ångström exponent of black carbon: from numerical aspects, Atmospheric Chemistry and Physics, 18, 6259–6273, 2018.

Liu, L. and Mishchenko, M.: Scattering and radiative properties of morphologically complex carbonaceous aerosols: a systematic modeling study, Remote Sensing, 10, 1634, 2018.

Liu, L. and Mishchenko, M. I.: Effects of aggregation on scattering and radiative properties of soot aerosols, Journal of Geophysical Research-Atmospheres, 110, <GotoISI>://WOS:000229988800009, 2005.

Luo, J.: Deriving_BrC_Revised.zip, https://doi.org/10.6084/m9.figshare.12839570.v1, https://figshare.com/articles/dataset/Deriving_BrC_Revised_zip/12839570, 2020.

Luo, J., Zhang, Y., Wang, F., Wang, J., and Zhang, Q.: Applying machine learning to estimate the optical properties of black carbon fractal aggregates, Journal of Quantitative Spectroscopy and Radiative Transfer, 215, 1–8, 2018a.

https://doi.org/10.5194/gmd-2020-348
Preprint. Discussion started: 5 November 2020

Luo, J., Zhang, Y., Wang, F., and Zhang, Q.: Effects of brown coatings on the absorption enhancement of black carbon: a numerical investigation, Atmospheric Chemistry and Physics, 18, 16 897–16 914, https://doi.org/10.5194/acp-18-16897-2018, https://www.atmos-chem-phys.net/18/16897/2018/, 2018b.

Luo, J., Zhang, Q., Luo, J., Liu, J., Huo, Y., and Zhang, Y.: Optical Modeling of Black Carbon With Different Coating Materials: The Effect of Coating Configurations, Journal of Geophysical Research: Atmospheres, 124, https://doi.org/10.1029/2019JD031701, https://agupubs.onlinelibrary.wiley.com/doi/abs/10.1029/2019JD031701, 2019.

Luo, J., Zhang, Y., and Zhang, Q.: The Ångström Exponent and Single-Scattering Albedo of Black Carbon: Effects of Different Coating Materials, Atmosphere, 11, https://doi.org/10.3390/atmos11101103, https://www.mdpi.com/2073-4433/11/10/1103, 2020.

Mackowski, D. W. and Mishchenko, M. I.: Calculation of the T matrix and the scattering matrix for ensembles of spheres, Journal of the Optical Society of America a-Optics Image Science and Vision, 13, 2266–2278, <GotoISI>://WOS:A1996VP77000015, 1996.

Mackowski, D. W. and Mishchenko, M. I.: A multiple sphere T-matrix Fortran code for use on parallel computer clusters, Journal of Quantitative Spectroscopy and Radiative Transfer, 112, 2182–2192, <GotoISI>://WOS:000294518300013, 2011.

Massabò, D., Caponi, L., Bernardoni, V., Bove, M., Brotto, P., Calzolai, G., Cassola, F., Chiari, M., Fedi, M., Fermo, P., et al.: Multi-wavelength optical determination of black and brown carbon in atmospheric aerosols, Atmospheric Environment, 108, 1–12, 2015.

Mishchenko, M. I. and Yurkin, M. A.: On the concept of random orientation in far-field electromagnetic scattering by nonspherical particles, Optics letters, 42, 494–497, 2017.

Mishchenko, M. I., Travis, L. D., and Lacis, A. A.: Scattering, absorption, and emission of light by small particles, Cambridge university press, 2002.

Nakayama, T., Sato, K., Matsumi, Y., Imamura, T., Yamazaki, A., and Uchiyama, A.: Wavelength and NO_x dependent complex refractive index of SOAs generated from the photooxidation of toluene, Atmospheric Chemistry and Physics, 13, 531–545, https://doi.org/10.5194/acp-13-531-2013, https://acp.copernicus.org/articles/13/531/2013/, 2013.

Russell, P., Bergstrom, R., Shinozuka, Y., Clarke, A., DeCarlo, P., Jimenez, J., Livingston, J., Redemann, J., Dubovik, O., and Strawa, A.: Absorption Ångström exponent Exponent in AERONET and related data as an indicator of aerosol composition, Atmospheric Chemistry and Physics, 10, 1155–1169, 2010.

Saleh, R., Hennigan, C. J., McMeeking, G. R., Chuang, W. K., Robinson, E. S., Coe, H., Donahue, N. M., and Robinson, A. L.: Absorptivity of brown carbon in fresh and photo-chemically aged biomass-burning emissions, Atmospheric Chemistry and Physics, 13, 7683–7693, https://doi.org/10.5194/acp-13-7683-2013, https://www.atmos-chem-phys.net/13/7683/2013/, 2013.

Saleh, R., Marks, M., Heo, J., Adams, P. J., Donahue, N. M., and Robinson, A. L.: Contribution of brown carbon and lensing to the direct radiative effect of carbonaceous aerosols from biomass and biofuel burning emissions, Journal of Geophysical Research: Atmospheres, 120, 10,285–10,296, https://doi.org/10.1002/2015JD023697, https://agupubs.onlinelibrary.wiley.com/doi/abs/10.1002/2015JD023697, 2015.

Schnaiter, M., Horvath, H., Mohler, O., Naumann, K. H., Saathoff, H., and Schock, O. W.: UV-VIS-NIR spectral optical properties of soot and soot-containing aerosols, Journal of Aerosol Science, 34, 1421–1444, <GotoISI>://WOS:000185856300007, 2003.

Srinivas, B., Rastogi, N., Sarin, M., Singh, A., and Singh, D.: Mass absorption efficiency of light absorbing organic aerosols from source region of paddy-residue burning emissions in the Indo-Gangetic Plain, Atmospheric environment, 125, 360–370, 2016.

Stocker, T. F., Qin, D., Plattner, G.-K., Tignor, M., Allen, S. K., Boschung, J., Nauels, A., Xia, Y., Bex, V., Midgley, P. M., et al.: Climate change 2013: The physical science basis, 2013.

https://doi.org/10.5194/gmd-2020-348
Preprint. Discussion started: 5 November 2020

Tesche, M., Müller, D., Gross, S., Ansmann, A., Althausen, D., Freudenthaler, V., Weinzierl, B., Veira, A., and Petzold, A.: Optical and microphysical properties of smoke over Cape Verde inferred from multiwavelength lidar measurements, Tellus B: Chemical and Physical Meteorology, 63, 677–694, https://doi.org/10.1111/j.1600-0889.2011.00549.x, https://doi.org/10.1111/j.1600-0889.2011.00549.x, 2011.

Wang, J., Nie, W., Cheng, Y., Shen, Y., Chi, X., Wang, J., Huang, X., Xie, Y., Sun, P., Xu, Z., et al.: Light absorption of brown carbon in eastern China based on 3-year multi-wavelength aerosol optical property observations and an improved absorption Ångström exponent segregation method, Atmospheric Chemistry and Physics, 18, 9061–9074, 2018.

Wang, X., Heald, C. L., Sedlacek, A. J., Sá, S. S. d., Martin, S. T., Alexander, M. L., Watson, T. B., Aiken, A. C., Springston, S. R., and Artaxo, P.: Deriving brown carbon from multiwavelength absorption measurements: method and application to AERONET and Aethalometer observations, Atmospheric Chemistry and Physics, 16, 12 733–12 752, 2016.

Wang, Y. Y., Liu, F. S., He, C. L., Bi, L., Cheng, T. H., Wang, Z. L., Zhang, H., Zhang, X. Y., Shi, Z. B., and Li, W. J.: Fractal Dimensions and Mixing Structures of Soot Particles during Atmospheric Processing, Environmental Science and Technology Letters, 4, 487–493, <GotoISI>://WOS:000415913800008, 2017.

Woźniak, M.: Characterization of nanoparticle aggregates with light scattering techniques, Theses, Aix-Marseille Université, https://tel.archives-ouvertes.fr/tel-00747711, 2012.

Yuan, Q., Xu, J., Wang, Y., Zhang, X., Pang, Y., Liu, L., Bi, L., Kang, S., and Li, W.: Mixing state and fractal dimension of soot particles at a remote site in the southeastern Tibetan plateau, Environmental science & technology, 53, 8227–8234, 2019.

Zhang, R. Y., Khalizov, A. F., Pagels, J., Zhang, D., Xue, H. X., and McMurry, P. H.: Variability in morphology, hygroscopicity, and optical properties of soot aerosols during atmospheric processing, Proceedings of the National Academy of Sciences of the United States of America, 105, 10 291–10 296, <GotoISI>://WOS:000258211600006, 2008.

Zhang, X., Mao, M., and Tang, S.: The absorption Ångström exponent exponent of black carbon with brown coatings: effects of aerosol microphysics and parameterization, Atmospheric Chemistry and Physics Discussions, 2020, 1–23, https://doi.org/10.5194/acp-2020-224, https://www.atmos-chem-phys-discuss.net/acp-2020-224/, 2020.

https://doi.org/10.5194/gmd-2020-348
Preprint. Discussion started: 5 November 2020

Geoscientific Model Development Discussions
Open Access
EGU

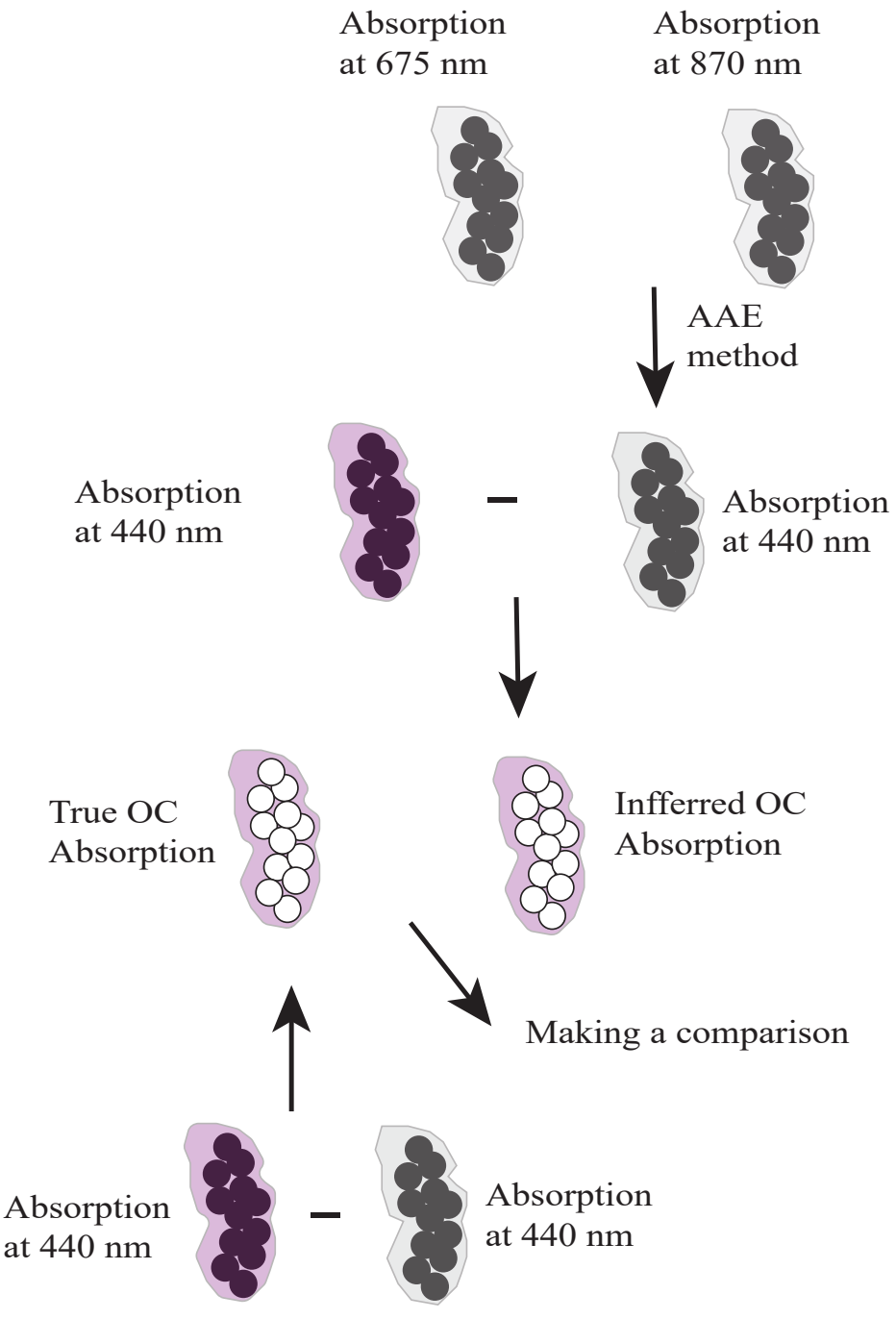

Figure 1. The estimation of BrC absorption.

https://doi.org/10.5194/gmd-2020-348
Preprint. Discussion started: 5 November 2020

Geoscientific Model Development Discussions
Open Access
EGU

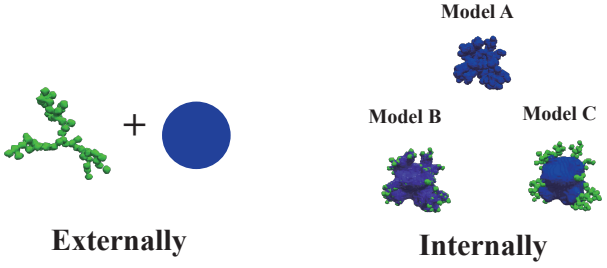

Figure 2. BC morphologies considered in this work. The internally mixed particles were generated using the models developed by Luo et al. (2019).

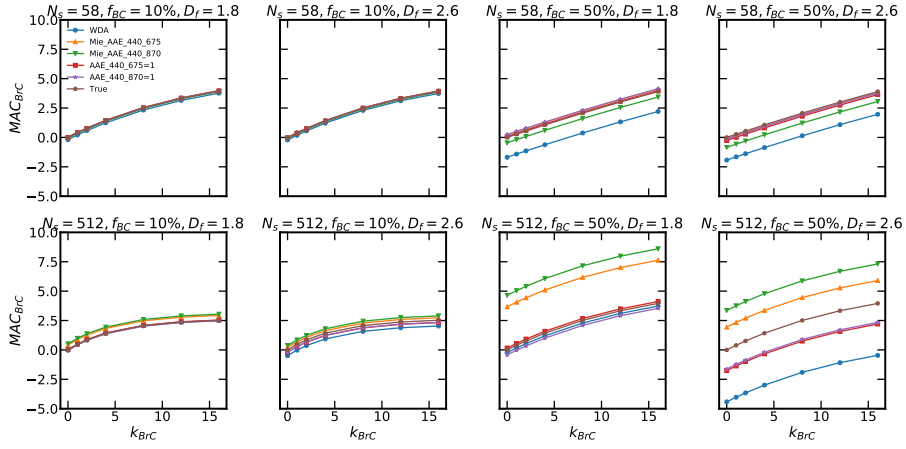

Figure 3. Comparison of the "True" and inferred BrC MAC, $\lambda = 440$ nm.

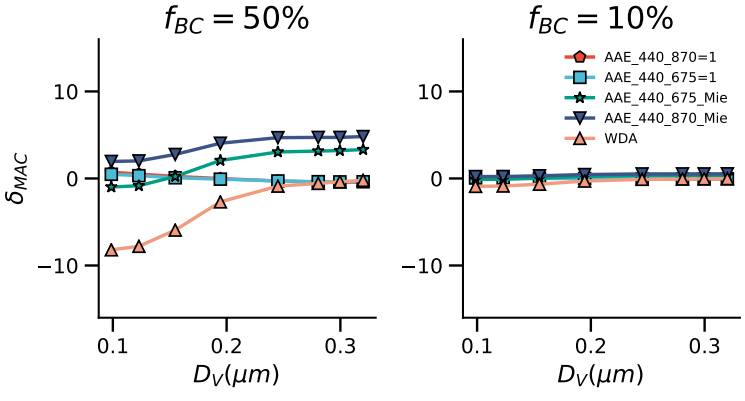

Figure 4. δ_{MAC} of inferred and "Ture" BrC absorption, and here D_V represents the equivalent volume size of BC, $\lambda = 440$ nm, D_f=1.8.

https://doi.org/10.5194/gmd-2020-348
Preprint. Discussion started: 5 November 2020

Geoscientific Model Development
Discussions
Open Access
EGU

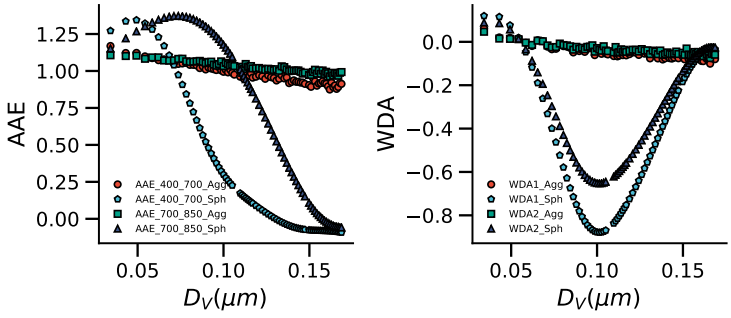

Figure 5. Comparison of AAE and WDA between BC sphere and aggregates (D_f=1.8, $m = 1.95 + 0.79i$).

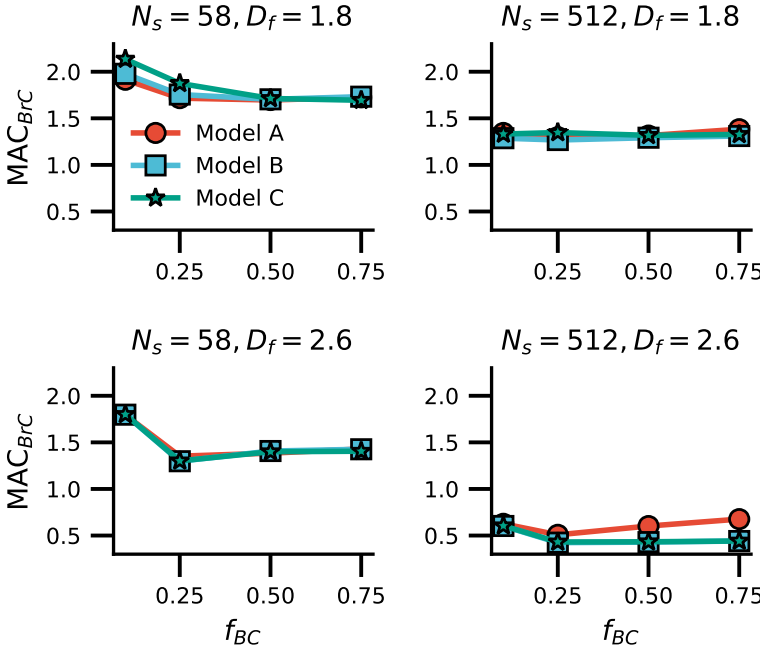

Figure 6. Variation of the "True" BrC absorption with different coating models, k_{BrC}=0.08, $\lambda = 440$ nm.

https://doi.org/10.5194/gmd-2020-348
Preprint. Discussion started: 5 November 2020

Geoscientific Model Development
Discussions
Open Access
EGU

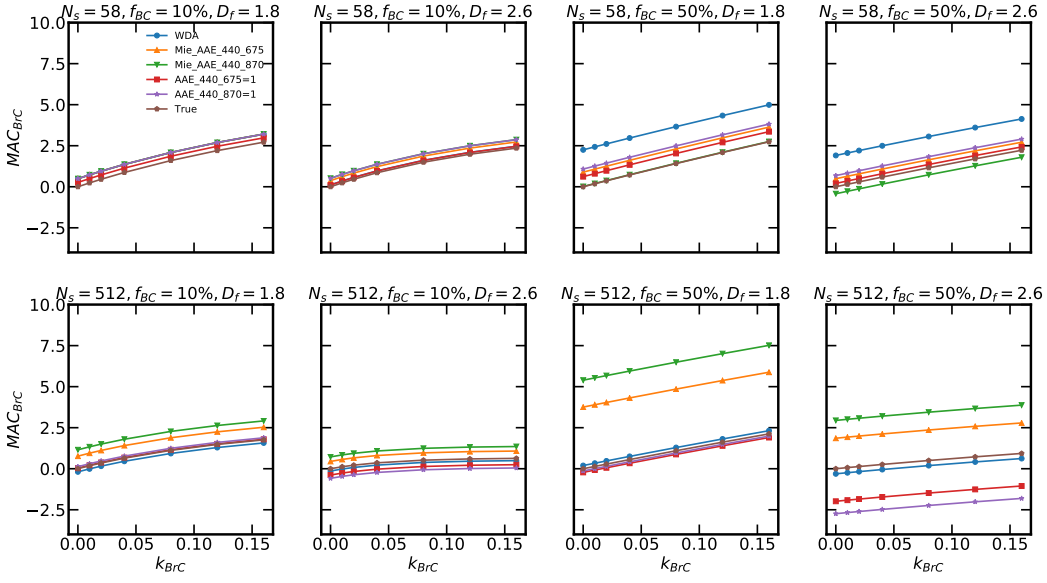

Figure 7. Comparison of the "True" and inferred BrC absorption for internally mixed particles (Model A), $\lambda = 440$ nm.

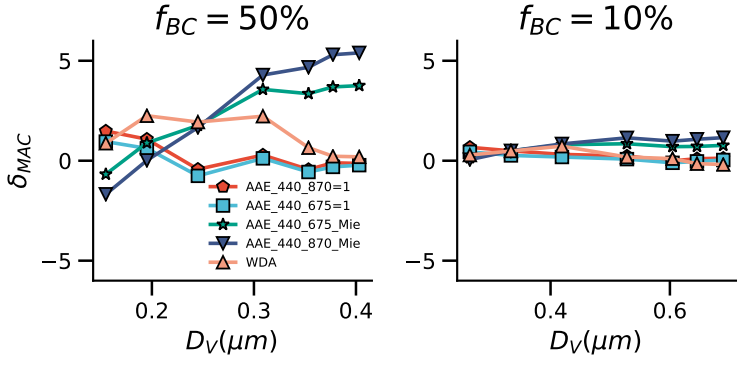

Figure 8. Similar as Figure 4, but for internally mixed particles ($D_f = 1.8$), $\lambda = 440$ nm.

https://doi.org/10.5194/gmd-2020-348
Preprint. Discussion started: 5 November 2020

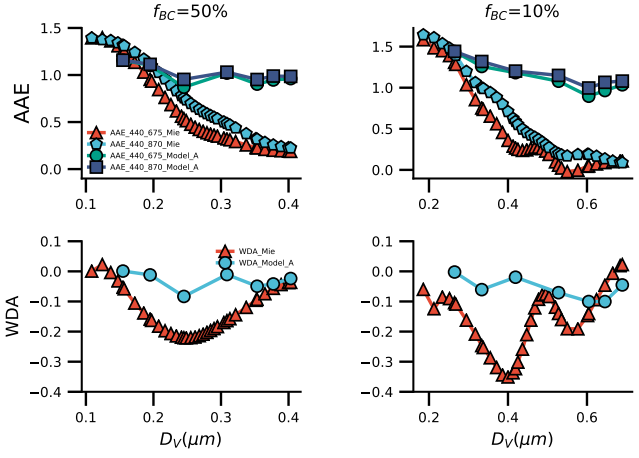

Figure 9. Comparison of AAE and WDA between core-shell sphere model and Model A.